Journal of the Optical Society of America B
OPTICAL PHYSICS

Raman converter of noisy double-scale pulses into coherent pulses

A. Kokhanovskiy, S. Smirnov, and S. Kobtsev*

Department of Laser Physics and Innovative Technologies, Novosibirsk State University, Pirogova St., 2, Novosibirsk 630090, Russia
*Corresponding author: sergey.kobtsev@gmail.com

Received 27 May 2020; revised 7 July 2020; accepted 7 July 2020; posted 8 July 2020 (Doc. ID 398581); published 31 July 2020

We propose and analyze a new mechanism for conversion of noise-like pulses into coherent ones with the help of a Raman process. The conditions that ensure conversion efficiency exceeding 45% were identified. Parameter ranges were established, within which the proposed mechanism can be implemented. We also define the condition of generation of stable Raman soliton molecules. The possibility of efficient conversion of noise-like pulses into coherent ones opens up new broad application fields for high-energy double-scale pulses.

https://doi.org/10.1364/JOSAB.398581

1. INTRODUCTION

Double-scale pulses are a class apart of optical pulses featuring a unique spectral–temporal structure of their electro-magnetic field [1,2]. These localized wave objects are composed of numerous subpicosecond pulses with randomly changing peak powers. Such wave packets are able to deliver record-high energy [3] directly from a master oscillator without any additional amplification. Double-scale pulses are also amenable to comparatively highly efficient nonlinear spectral conversion [4,5], their parameters span a great range of variability [6], and they can be fairly easily generated in many mode-locked fiber lasers with relatively long [7] and short [8,9] cavities. In spite of their incoherence or only partial coherence, these pulses (also termed noise-like pulses [1,10]) have found a number of applications [9,11,12]. However, these applications may be considerably broadened if an efficient mechanism of conversion from these stochastic pulses into “conventional” fully coherent laser pulses [13] is found.

Such mechanisms may be provided by processes where double-scale pulses play the role of efficient transfer agent for electromagnetic energy with its final conversion into conventional coherent single-scale pulses carrying high energy. One such process is stimulated Raman scattering in optical fiber. It was recently shown that a Raman laser with an artificial saturable absorber (NOLM [14]) can be used for conversion of incoherent radiation from an ASE source into picosecond pulses without stochastic subpulses [15].

It should be pointed out that Raman lasers allow independence of the converted radiation structure from that of the pumping pulses. Without mode-locking elements in the Raman cavity, the converted pulses copy the pumping ones [16–18]. Consequently, when noisy double-scale pulses are used for pumping, the generated Raman output contains the same type of noisy double-scale pulses.

The present work, for the first time to the best of our knowledge, discusses mechanisms of conversion of incoherent double-scale pulses into conventional coherent single-scale optical pulses. In the following, we numerically studied a Raman converter with spectral filtration and saturable absorption as crucial effects leading to mode-locking. The paper also aims to find conditions under which fluctuations of double-scale pulses may be mitigated within converted pulses inside a fiber cavity.

2. CONCEPT

Since stimulated Raman scattering is insensitive to pump phase, i.e., a new (Stokes) wave arises without being phase-locked to the pump wave, the generated wave and pumping may thus have different types of coherence and different pulse structure. To date, several examples of such conversion have been reported: CW amplified spontaneous emission used as the pump radiation was converted into Raman dissipative solitons [19], whereas coherent picosecond pumping pulses were converted into double-scale pulses [20]. The present work studies the possibility of an opposite transformation as compared with [20], namely, the prospect of conversion from double-scale (incoherent) pumping pulses into coherent Raman solitons. It is pertinent to recall that the problem of coherence improvement is a general one, and one of its well-known and often used solutions works through pumping of an active medium with radiation that generates output with better coherence. This is the case of lasers and amplifiers pumped with multimode radiation, as a result of which single-mode radiation may be generated/amplified. It is also well known that an active medium pumped with multifrequency radiation may generate/amplify single-frequency radiation.

This work reports the results of modelling of the possibilities of efficient conversion of noisy double-scale pulses into coherent ones in a synchronously pumped Raman fiber laser with saturable absorption.

3. PROPOSED CONFIGURATION

Shown in Fig. 1 is a schematic diagram of the proposed configuration for conversion from noisy double-scale pulses to coherent output. Launched double-scale pulses induce formation of Raman pulses propagating in the same direction.

In the proposed configuration, noisy double-scale pulses are used for synchronous pumping of a ring cavity containing a Raman fiber (for instance, P_2O_5-doped fiber) as well as saturable absorber and a spectral filter. There is one fundamental property that the saturable absorber must possess: it has to be relatively fast, i.e., its recovery time must be shorter than the round-trip time of the Raman laser cavity. Such saturable absorbers are not unusual because the required short recovery time normally accompanies fast nonradiative relaxation in the absorbing medium [21].

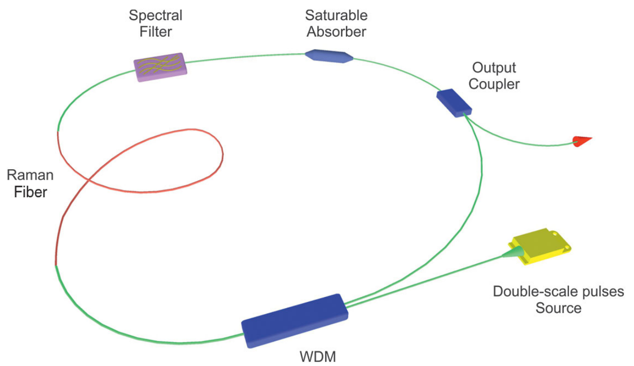

Fig. 1. Schematic diagram of the synchronously pumped Raman convertor with a saturable absorber and a spectral filter.

The length of the Raman convertor cavity was chosen equal to 20 m, which is close to the experimental setup of the work [17]. In comparison with this work, we have added a spectral filter and a saturable absorber to achieve mode locking. The used spectral filter has a flat-top sixth-order super Gaussian profile. The spectral filter bandwidth can be adjusted in our simulations for optimization purposes. Transmittance of the fast saturable absorber is given by Eq. (1):

$$T = 1 - \frac{L_{\text{unsat}}}{1 + P/P_{\text{sat}}}, \tag{1}$$

where L_{unsat} = unsaturated losses and P_{sat} = saturation power of the saturable absorber.

Double-scale pulses were modelled as a superposition of uncoherent longitudinal modes of the laser cavity:

$$A(t) = \sqrt{P(t)} \cdot \sum_j A_j \exp\left(-i\omega_j t\right), \tag{2}$$

where A denotes the complex amplitude of the double-scale pulse, ω_j and A_j are frequency and complex amplitude of the jth longitudinal mode of the laser cavity, t stands for time, and temporal envelope $P(t)$ of the simulated wave-packets was chosen in the following form:

$$P(t) = \frac{P_0}{\cosh^2\left(\frac{t}{\tau}\right)}, \tag{3}$$

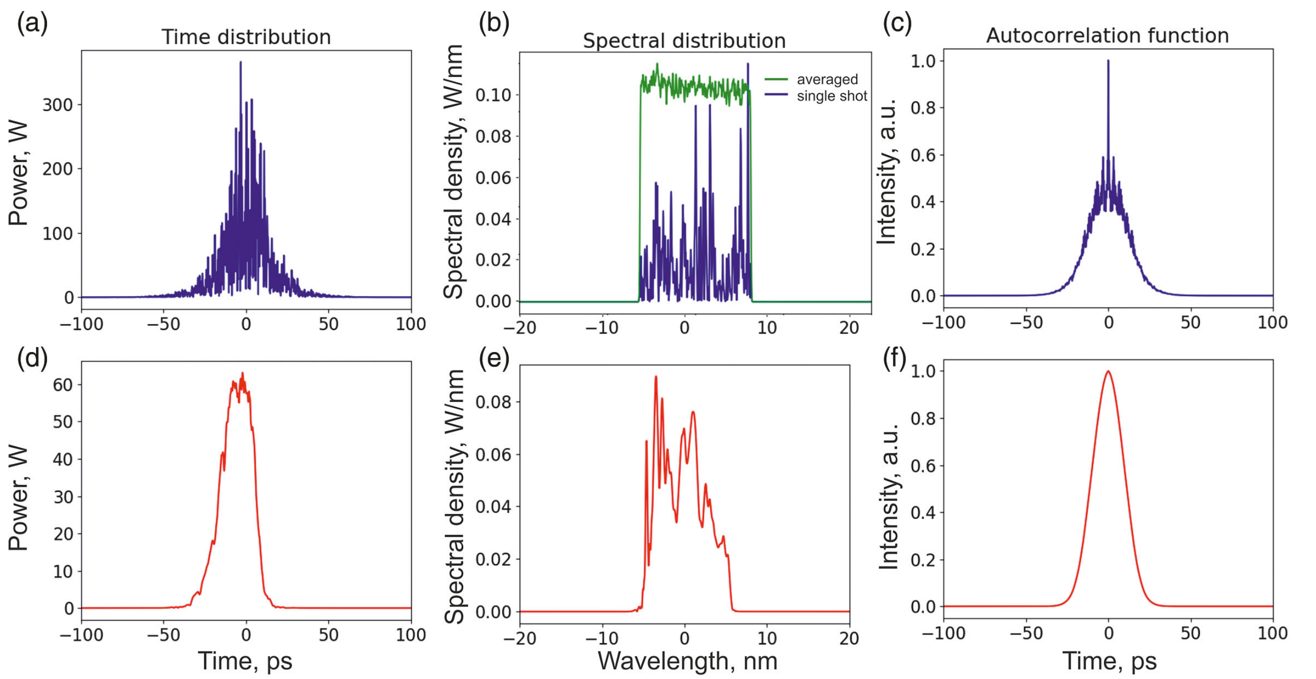

Fig. 2. Upper row: temporal and spectral distribution; autocorrelation function of a seed double-scale pulse. Bottom row: temporal and spectral distribution; autocorrelation function of the corresponding Raman pulse.

where τ stands for pulse duration and P_0 denotes peak power of the pulse. For simplicity, we used constant amplitudes $|A_j| = 1$ and uniformly distributed in the range $(0, 2\pi)$ random phases arg A_j of spectral modes within the optical spectrum of double-scale pulses, although more sophisticated models could consider fluctuations of mode amplitudes that result in bell-shaped spectra typical for double-scale pulses [2,3,22–24].

As pumping radiation in modelling, we used double-scale pulses with 30 ps envelope duration and 330 fs duration of subpulses and 12.6 nm spectral bandwidth [Figs. 2(a)–2(c)]. Similar pulses may be generated, for instance, in a figure-8 laser [25].

Adequate modelling of synchronized pumping requires new initialization of double-scale pulses at each cavity round-trip. This procedure leads to energy fluctuation of pumping pulses due to intrinsic stochasticity of incoherent modes composing the pulse. Averaging of double-scale pulses over a millisecond scale, which is typical for common radiation power meters, results in 1.6% relative fluctuation of pumping pulse energy.

In order to simulate nonlinear propagation of laser pulses along optical fibers, while considering Raman scattering, the generalized nonlinear Schrödinger equation is widely used [26]:

$$\partial_z A = -\frac{i\beta_2}{2}\partial_t^2 A + i\gamma\left(1 + \frac{i\partial_t}{\omega_0}\right) \times \left(A\int_0^\infty R\left(t'\right)\left|A\left(z, t, -t'\right)\right|^2 \mathrm{d}t'\right), \quad (4)$$

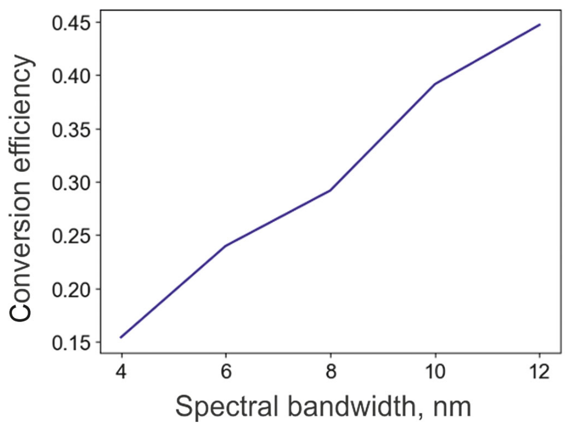

Fig. 3. Conversion efficiency of Raman converter against bandwidth of a spectral filter.

where $A(z, t)$ stands for the complex field envelope; z and t are the longitudinal coordinate and time in the retarded frame of reference; ω_0 stands for the carrier frequency; β_2 and γ are the dispersion and nonlinear coefficients; c denotes the light speed in vacuum; $i^2 = -1$. We used the following values of nonlinear and dispersion coefficients in our simulations: $\gamma = 4.7$ $(\mathrm{W\,km})^{-1}$ and $\beta_2 = 1.4 \times 10^{-26}$ $\mathrm{sec}^2/\mathrm{m}$. The kernel $R(t)$ of the integral operator includes both electronic (instantaneous) and nuclear contributions: $R(t) = (1 - f_R)\delta(t) + f_R h_R(t)$. Delayed (Raman) response of silica $h_R(t)$ in the first approximation can be taken in the form of a damped oscillator [20]. Due to a short length of the Raman oscillator, we neglected the linear losses of the optical fiber. In order to speed up numerical simulations, we also used approximation of slowly varied amplitudes for Eq. (4), as described in [27].

4. RESULTS

During the first stage, we perform a search in a sparse grid of parameters. The first mode-locked regime was obtained at the following parameters of the fiber laser cavity: cavity length $L = 20$ m, spectral filter bandwidth: 9 nm, saturable absorber $P_{\mathrm{sat}} = 30$ W, $L_{\mathrm{unsat}} = 0.1$, coupler ratio $\alpha = 0.4$. The average energy of the pumping double-scale pulse was 1.2 nJ, while the energy of the converted pulse was 0.37 nJ. Figure 2 depicts a pump pulse at the beginning of the Raman convertor and a Raman pulse at the output of the Raman convertor.

Phases of different uncoherent subpulses of pumping pulses locking inside a Raman oscillator may be observed on temporal and spectral distributions of converted Raman pulses. Disappearance of the coherence spike in the autocorrelation function of the Raman pulse shown in Fig. 2(f) indicates a mode-locked state.

The first set of Raman convertor parameters supports a mode-locking effect up to 1.5 nJ energy of pumping pulses. Raising the pumping pulse energy above this threshold leads to destabilization of the mode-locked state.

Our next step was to investigate the influence of different elements of a Raman converter in order to improve its efficiency and raise the supported energy of pumping pulses.

A. Spectral Filtering Effect

Spectral filter bandwidth introduces losses to the Raman pulses during propagation through the filter. Therefore, the conversion efficiency may be improved by applying a broadband spectral

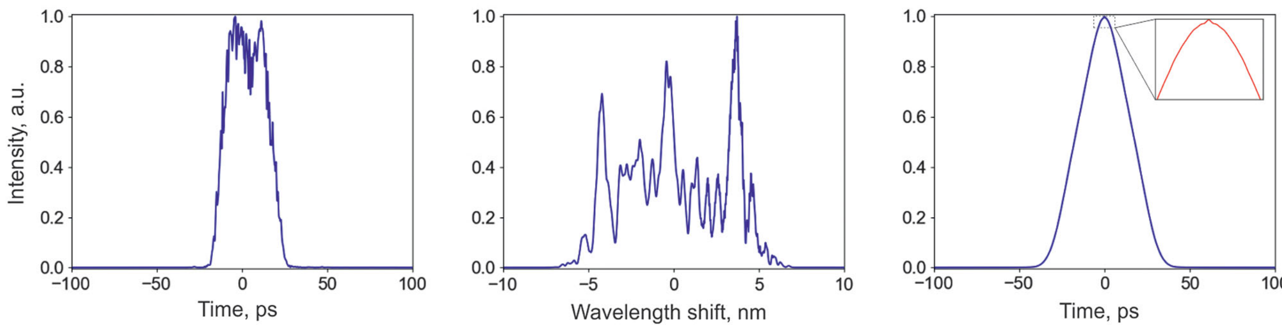

Fig. 4. Raman pulse resulting from 10 nm bandwidth filtering.

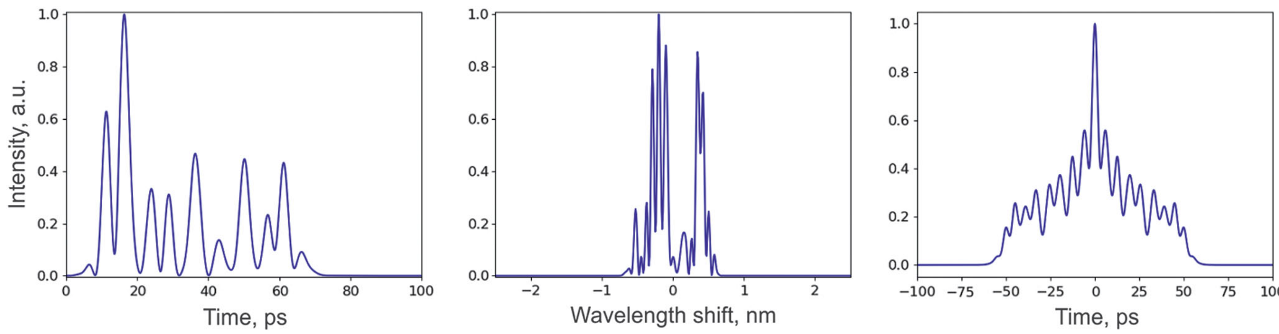

Fig. 5. Raman soliton molecule resulting from 1 nm bandwidth filtering.

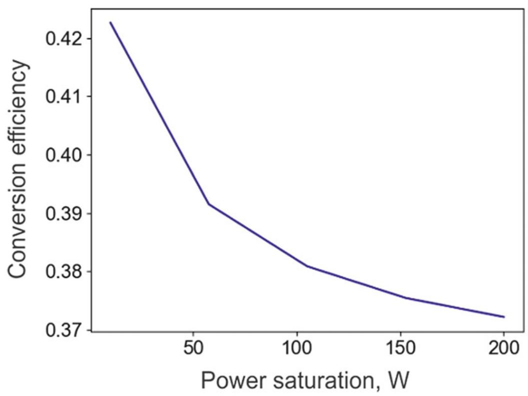

Fig. 6. Conversion efficiency and peak power of the converted Raman pulses versus saturation power of saturable absorber.

filter (Fig. 3). Broader spectral bandwidth also affects threshold energy of pumping pulses supporting stable mode-locking regimes. However, we observed appearance of a small coherence peak in the autocorrelation function of the Raman pulse after reaching the energy of 3.5 nJ in the pumping pulse with a spectral filter wider than 10 nm (Fig. 4).

Insertion of a spectral filter into the Raman cavity may significantly affect the properties of conversion from noisy double-scale pulses into coherent ones and, therefore, produce considerable changes in the parameters of output pulses. Specifically, the presence of a narrow spectral filter with a 1 nm bandwidth results in formation of Raman soliton molecules composed of solitons with different intensities (Fig. 5). In order to avoid this effect, which may be undesirable in most practical cases, wider spectral filters should be used.

B. Saturable Absorption Effect

Unsaturated losses of the saturable absorber have a dramatic impact on conversion efficiency of the Raman converter and therefore should be minimized. Additionally, low values of unsaturated losses also reduce the influence of the saturation power. The saturation power that may be associated with nonlinear loses only slightly affects the efficiency and peak power of the converted Raman pulses (Fig. 6).

C. Cavity Length Effect

Despite achieving a mode-locked state, we observe strong energy fluctuations of the output Raman pulses per round-trip induced by energy fluctuations of the input double-scale pulses (Fig. 7). To mitigate this effect, we propose elongation of the Raman convertor. Elongation increases interaction time between pumping and Raman pulses and, therefore, increases the averaging effect of stimulated Raman scattering.

To characterize energy fluctuations, we use normalized standard deviation (NSTD) of the energy calculated as follows:

$$\mathrm{NSTD} = \frac{\sqrt[2]{(E_i - E)^2}}{E}, \quad (5)$$

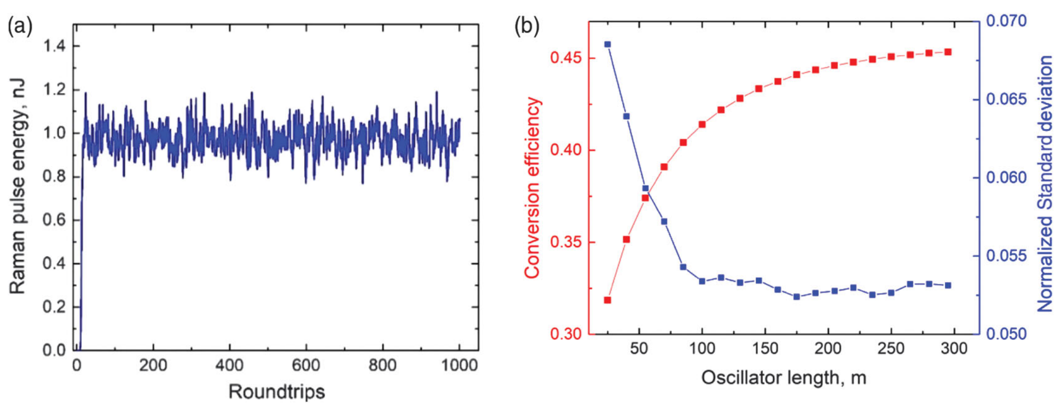

Fig. 7. (a) Energy evolution of converted double-scale pulses. (b) Conversion efficiency and normalized standard deviation versus length of the Raman convertor.

where E_i = energy of the Raman pulse after the ith roundtrip, and E = mean energy of the Raman pulse.

Extending the Raman convertor from 20 to 300 m led to the NSTD of the output energy dropping from 0.068 to 0.053. It also increased the conversion efficiency due to a longer interaction length.

5. CONCLUSION

We demonstrated, for the first time to the best of our knowledge, the possibilities of the proposed mechanism of conversion from incoherent noise-like pulses to coherent pulses through transformation in Raman fiber laser. It was shown that the conversion efficiency may exceed 45%. Also, the conversion properties were studied depending on the spectral filtration of Raman pulses. The conditions were established leading to formation of Raman soliton molecules, which constitutes an undesirable effect in the proposed concept. Efficient conversion of incoherent noise-like pulses into coherent ones opens up greater opportunities of practical application of noisy double-scale laser pulses.

Funding. Russian Science Foundation (17-12-01281).

Disclosures. The authors declare no conflicts of interest.

REFERENCES

1. M. Horowitz, Y. Barad, and Y. Silberberg, "Noiselike pulses with a broadband spectrum generated from an erbium-doped fiber laser," Opt. Lett. **22**, 799–801 (1997).
2. S. Kobtsev, S. Kukarin, S. Smirnov, S. Turitsyn, and A. Latkin, "Generation of double-scale femto/pico-second optical lumps in mode-locked fiber lasers," Opt. Express **17**, 20707–20713 (2009).
3. A. Ivanenko, S. Kobtsev, S. Smirnov, and A. Kemmer, "Mode-locked long fibre master oscillator with intra-cavity power management and pulse energy > 12 μJ," Opt. Express **24**, 6650–6655 (2016).
4. S. V. Smirnov, S. M. Kobtsev, and S. V. Kukarin, "Efficiency of non-linear frequency conversion of double-scale pico-femtosecond pulses of passively mode-locked fiber laser," Opt. Express **22**, 1058–1064 (2014).
5. H. Xia, H. Li, G. Deng, J. Li, S. Zhang, and Y. Liu, "Compact noise-like pulse fiber laser and its application for supercontinuum generation in highly nonlinear fiber," Appl. Opt. **54**, 9379–9384 (2015).
6. S. V. Smirnov, S. M. Kobtsev, and S. K. Turitsyn, "Wide variability of generation regimes in mode-locked fiber lasers," in *Shaping Light in Nonlinear Optical Fibers*, S. Boscolo and C. Finot, eds. (Wiley, 2017), p. 415.
7. S. Kobtsev, S. Kukarin, and Y. Fedotov, "Ultra-low repetition rate mode-locked fiber laser with high-energy pulses," Opt. Express **16**, 21936–21941 (2008).
8. J. Lin, C. Chen, C. Chan, W. Chang, and Y. Chen, "Investigation of noise-like pulses from a net normal Yb-doped fiber laser based on a nonlinear polarization rotation mechanism," Opt. Lett. **41**, 5310–5313 (2016).
9. V. Voropaev, A. Donodin, A. Voronets, D. Vlasov, V. Lazarev, M. Tarabrin, and A. Krylov, "Generation of multi-solitons and noise-like pulses in a high-powered thulium-doped all-fiber ring oscillator," Sci. Rep. **9**, 18369 (2019).
10. G. M. Donovan, "Dynamics and statistics of noise-like pulses in mod-elocked lasers," Physica D **309**, 1–8 (2015).
11. G. Parker, D. Parker, B. Nie, V. Lozovoya, and M. Dantus, "Laser-induced breakdown spectroscopy and ablation threshold analysis using a megahertz Yb fiber laser oscillator," Spectrochim. Acta B **107**, 146–151 (2015).
12. C.-L. Pan, A. Zaytsev, Y.-J. You, and C.-H. Lin, "Fiber-laser-generated noise-like pulses and their applications," in *Fiber Laser*, M. Paul, ed. (InTech, 2016).
13. Y. Song, X. Shi, C. Wu, D. Tang, and H. Zhang, "Recent progress of study on optical solitons in fiber lasers," Appl. Phys. Rev. **6**, 021313 (2019).
14. N. J. Doran and D. Wood, "Nonlinear-optical loop mirror," Opt. Lett. **13**, 56–58 (1988).
15. W. Pan, J. Zhou, L. Zhang, and Y. Feng, "Raman dissipative soliton fiber laser mode locked by a nonlinear optical loop mirror," Opt. Express **27**, 17905–17911 (2019).
16. S. Kobtsev, S. Kukarin, S. Smirnov, and I. Ankudinov, "Cascaded SRS of single- and double-scale fiber laser pulses in long extra-cavity fiber," Opt. Express **22**, 20770–20775 (2014).
17. W. C. Chang, J. H. Lin, T. Y. Liao, and C. Y. Yang, "Characteristics of noise-like pulse with broad bandwidth based on cascaded Raman scattering," Opt. Express. **26**, 31808–31816 (2018).
18. S. Kobtsev, A. Ivanenko, A. Kokhanovsky, and M. Gervaziev, "Raman-converted high-energy double-scale pulses at 1270 nm in P_2O_5-doped silica fiber," Opt. Express **26**, 29867–29872 (2018).
19. W. Pan, L. Zhang, J. Zhou, X. Yang, and Y. Feng, "Raman dissipative soliton fiber laser pumped by an ASE source," Opt. Lett. **42**, 5162–5165 (2017).
20. E. A. Golovchenko, E. M. Dianov, P. V. Mamyshev, A. M. Prokhorov, and D. G. Fursa, "Theoretical and experimental study of syn-chronously pumped dispersion-compensated femtosecond fiber Raman lasers," J. Opt. Soc. Am. B **7**, 172–181 (1990).
21. F. X. Kartner, J. Aus der Au, and U. Keller, "Mode-locking with slow and fast saturable absorbers—what's the difference?" IEEE J. Sel. Top. Quantum Electron. **4**, 159–168 (1998).
22. Y. Jeong, L. A. Vazquez-Zuniga, S. Lee, and Y. Kwon, "On the formation of noise-like pulses in fiber ring cavity configurations," Opt. Fiber Technol. **20**, 575–592 (2014).
23. J. P. Lauterio-Cruz, H. E. Ibarra-Villalon, O. Pottiez, Y. E. Bracamontes-Rodriguez, O. S. Torres-Muñoz, J. C. Hernandez-Garcia, and H. Rostro-Gonzalez, "Numerical study of complex dynamics and extreme events within noise-like pulses from an erbium figure-eight laser," Opt. Express **27**, 37196–37213 (2019).
24. S. Smirnov, S. Kobtsev, S. Kukarin, and A. Ivanenko, "Three key regimes of single pulse generation per round trip of all-normal-dispersion fiber lasers mode-locked with nonlinear polarization rotation," Opt. Express **20**, 27447–27453 (2012).
25. A. Kokhanovskiy, A. Ivanenko, S. M. Kobtsev, and S. Turitsyn, "Coherence automatic adjustment of the optical pulses inside mode-lock fiber laser cavity," Proc. SPIE **10825**, 1082518 (2018).
26. D. Wood and K. J. Blow, "Theoretical description of transient stimulated Raman scattering in optical fibers," IEEE J. Quantum Electron. **25**, 2665–2673 (1989).
27. S. V. Smirnov, "Efficient numerical model of stimulated Raman scattering in optical fibers," J. Opt. Soc. Am. B **37**, 1219–1223 (2020).